

Elastic Scattering of Intermediate-Energy Alpha Particles by Heavy Nuclei*

GEORGE W. FARWELL AND HARVEY E. WEGNER†

Department of Physics, University of Washington, Seattle, Washington

(Received May 24, 1954)

The deflected alpha-particle beam of the University of Washington 60-inch cyclotron has been used to study the elastic scattering of 13- to 42-Mev alpha particles by Ag, Ta, Pb, and Th at 60°. The alpha-particle energy was decreased in steps of approximately 1 Mev by placing remotely controlled absorbers in the cyclotron beam. Elastically scattered alpha particles were selected and counted by a differential-range coincidence proportional-counter telescope.

Up to a certain critical energy E_0 , which increases with Z , the cross section for each element decreases with increasing alpha-particle energy in agreement with the Rutherford formula. At higher energies, the dependence is given by the empirical formula $\sigma(E) = \sigma(E_0) \exp\{-K(E-E_0)\}$. The slope parameter K is about 0.26 Mev^{-1} and decreases slightly as Z increases. Interpretation of results in terms of a semiclassical strong absorption model leads to values of the sum of nuclear radius and alpha-particle radius best fitted by the empirical formula $D = (1.50A^{1/3} + 1.4) \times 10^{-13} \text{ cm}$.

I. INTRODUCTION

THE first observation¹ of scattering of alpha particles through large angles led Rutherford² to suggest a nuclear structure for the atom. Subsequent experiments³⁻⁵ verified the predictions of Rutherford's theory with regard to the dependence of the scattering probability upon thickness of scatterer, alpha-particle energy, and scattering angle, and established the correspondence between nuclear charge and atomic number. Assuming classical trajectories for the scattered alpha particles, Coulomb's law was found to hold for encounters between alpha particles and nuclei for which the distances of closest approach, or apsidal distances, were as small as $3.2 \times 10^{-12} \text{ cm}$ (Au), $2.0 \times 10^{-12} \text{ cm}$ (Ag), and $1.2 \times 10^{-12} \text{ cm}$ (Cu).

The first evidence of departures from Coulomb's law, other than those observed in alpha scattering by H and He, was obtained by Bieler,⁶ who studied the angular distribution of Ra (B+C) alphas scattered by Mg and Al. For Al, the ratio of the observed scattering cross section to the Coulomb cross section, $\sigma/\sigma_{\text{Coul}}$, was found to decrease from 1.0 at small angles to about 0.6 at 110°. Rutherford and Chadwick,⁵ measuring the dependence of cross section upon alpha-particle energy, found in the case of Al that $\sigma/\sigma_{\text{Coul}}$ at 135° dropped from about 1 at apsidal distances greater than $13 \times 10^{-13} \text{ cm}$ to less than 0.4 at $7-8 \times 10^{-13} \text{ cm}$, increasing again to about 0.7 at $6 \times 10^{-13} \text{ cm}$. Similar results, but without the rise at very small apsidal distances, were observed for 90° scattering from Al. Extensive investigations in the non-Coulomb region were not feasible because of the limited range of alpha-particle energies available from natural alpha sources.

The 43-Mev alpha-particle beam of the University of Washington 60-inch cyclotron has been used in a recent series of experiments to measure cross section for elastic scattering by heavy nuclei as a function of alpha-particle energy, and considerable information has been obtained in the non-Coulomb region.

Results for 60° and 95° scattering by Au have been reported previously.⁷ The observed scattering cross section for Au follows the Rutherford dependence closely at low energies, but drops sharply as the alpha-particle energy increases above a well-defined "critical energy" which depends upon the scattering angle. The classical apsidal distance corresponding to the critical energy is considerably larger ($\sim 13 \times 10^{-13} \text{ cm}$) than the sum of the presently accepted values of the Au nuclear radius ($8-9 \times 10^{-13} \text{ cm}$) and the alpha-particle radius ($1-2 \times 10^{-13} \text{ cm}$). At energies above the critical energy E_0 , the dependence of cross section upon energy is well represented by the simple empirical formula $\sigma(E) = \sigma(E_0) \exp\{-K(E-E_0)\}$, where the coefficient K depends upon the scattering angle.

The present paper reports results obtained for elastic alpha-particle scattering by Ag, Ta, Pb, and Th. The dependence of cross section upon energy is in all cases similar to that for Au, although the critical energy E_0 and (to a much lesser degree) the coefficient K depend upon the atomic number of the scattering element. The results are interpreted in terms of a semiclassical strong absorption model due to Blair,⁸ and information obtained about nuclear and alpha-particle radii is presented.

II. APPARATUS AND EXPERIMENTAL METHOD

A schematic view of the apparatus used in the present experiments is shown in Fig. 1. The deflected alpha-particle beam of the 60-inch cyclotron enters the evacuated target box T. Part of the beam passes through a defining aperture A in plate B. Variable

* Partially supported by the U. S. Atomic Energy Commission.

† Now at Brookhaven National Laboratory, Upton, New York.

¹ H. Geiger and E. Marsden, Proc. Roy. Soc. (London) **A82**, 495 (1909).

² E. Rutherford, Phil. Mag. **21**, 669 (1911).

³ H. Geiger and E. Marsden, Phil. Mag. **25**, 604 (1913).

⁴ J. Chadwick, Phil. Mag. **40**, 734 (1920).

⁵ E. Rutherford and J. Chadwick, Phil. Mag. **50**, 889 (1925).

⁶ E. S. Bieler, Proc. Roy. Soc. (London) **A105**, 434 (1924).

⁷ George W. Farwell and Harvey E. Wegner, Phys. Rev. **93**, 356 (1954).

⁸ J. S. Blair, following paper, Phys. Rev. **95**, 1218 (1954).

absorbers C_1 and C_2 reduce the alpha-particle energy; energies from 43 Mev down to 13 Mev are available in intervals of about 1 Mev. The alpha particles enter the thin foil target D , most of them being transmitted to the Faraday cup E , the current to which is monitored by a beam current integrator. Alpha particles scattered through an angle of approximately 60° pass down tube F and out through a vacuum-tight thin foil exit window W . A system of variable aluminum absorbers J and a coincidence proportional-counter telescope K_1, K_2 serve as a differential range device, giving both the number and the range of the elastically scattered alpha particles. Studies of elastic scattering at angles other than 60° can be made by using tubes G and H , which are mounted at approximately 90° and 125° , respectively, to the incident beam.

At each value of the incident alpha-particle energy (i.e., for each configuration of absorbers C_1 and C_2) the number of alpha particles scattered elastically during a convenient time interval is observed with the counter telescope and normalized against the integrated beam current; at the same time, a mean range determination is made which yields the energy of the incident alpha particles. Thus relative elastic scattering cross section is obtained as a function of alpha-particle energy.

The water-cooled absorber C_1 is constructed of five layers of 0.35-mil copper foil arranged in a stepwise manner as shown in Fig. 1; each step is wider than the aperture A . Absorber C_2 is similar in construction, with individual copper foil thicknesses of 1.8 mils. The two absorbers may be moved across the aperture A by remote control, allowing the absorber thickness to be adjusted in steps of approximately 0.35 mil. Thus incident alpha-particle energies ranging from 43 Mev (no absorber) down to about 13 Mev (the minimum energy necessary for a range measurement in the detecting system) are available in steps of approximately 1 Mev.

The target foil D is preceded by a defining baffle (not shown) which prevents alpha particles scattered by absorbers C_1 and C_2 from registering on the Faraday cup E without traversing the target foil. The usual target thickness is about 0.3 mil.⁹

Since the entire target assembly is located within the fringing field of the cyclotron magnet, the trajectories of the scattered alpha particles are curved. The curvature depends upon alpha-particle energy, and it is difficult to determine the exact angle of scattering for each energy. Study of calculated trajectories indicates that for the "60°" case, the angle of scattering ranges from about 62° at 10 Mev to 59° at 40 Mev; 60° is the estimated value at the energies of primary interest (Sec. III).

⁹ Very uniform thin foils of a number of elements were obtained from Baker and Company, Inc., 113 Astor Street, Newark 5, New Jersey. The Pb foil was rolled in our laboratory. The Th foil, made by electrolytic methods, was kindly furnished by Professor F. H. Schmidt.

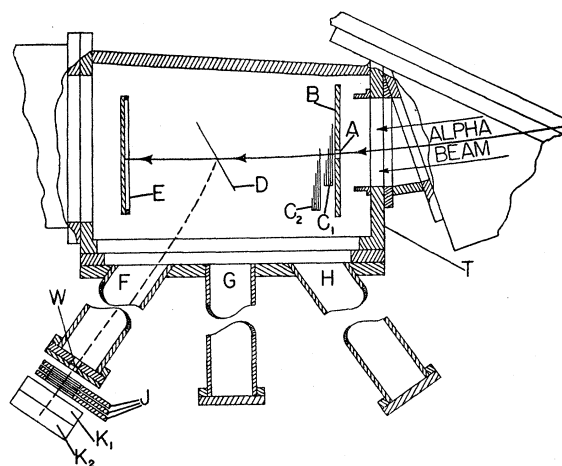


FIG. 1. Plan view (schematic) of scattering apparatus. A , aperture in plate B for defining the alpha-particle beam; C_1 and C_2 , remotely controlled absorbers for reducing beam energy; D , thin foil target; E , Faraday cup; F , G , and H , observation ports; W , thin foil exit window; J , variable aluminum absorber for differential-range proportional-counter telescope K_1, K_2 .

The variable aluminum absorber J consists of three remotely controlled foil wheels mounted on a common axis. Each foil wheel contains a series of Al foil stacks of increasing thickness mounted in equally spaced holes near its periphery. The position of each foil wheel can be controlled independently, so that total absorber thicknesses of from zero to 412 mg/cm^2 of Al, in steps of 1.2 mg/cm^2 , can be interposed between scattering foil and counters.

The proportional counters K_1 and K_2 are contained in a common envelope filled with argon at a pressure of about $\frac{1}{4}$ atmosphere. Collecting electrodes are 2-mil wolfram wires maintained at a positive potential of 800 volts.

Pulses from each counter pass through a well-shielded battery-operated preamplifier, located in the cyclotron room, to a linear amplifier and discriminator located in the control room. Discriminator outputs are fed to a coincidence circuit and scaler. The coincidence circuit requires that an alpha particle pass through both counter K_1 and counter K_2 in order to be registered. Proton pulses are biased out. Energy selectivity is adjusted by means of discriminator bias on the K_2 channel; the higher the bias, the more strict the requirement that the particle just end its range in counter K_2 , thus giving the maximum possible ionization in that counter.

Figure 2 shows a small part of the data for a typical run. Coincidence counting rate, normalized to the integrated beam current, is plotted against Al absorber thickness for each of several different beam energies. The elastic scattering cross section at each energy is proportional to the peak counting rate. The alpha-particle energy for a given peak is found by noting the Al absorber thickness at the peak and adding corrections for energy loss in the target foil, the exit window, the

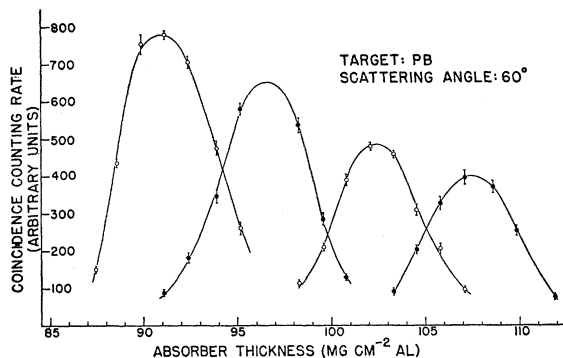


FIG. 2. Part of the data for a typical run (Pb). Normalized coincidence counting rate is plotted against Al absorber thickness (in the counter system) for each of several different beam energies. The elastic scattering cross section at each energy is proportional to the peak counting rate. The alpha-particle energy for each peak is found from the absorber thickness after addition of appropriate corrections (see text).

air path to the counter, and the counter itself. Total equivalent range in Al is then found and converted to energy by use of range-energy curves.¹⁰

The data plotted in Fig. 2 were taken with biases set for less-than-maximum energy selectivity. The average peak width (full width at half-maximum) is about 6 mg/cm²; at an alpha-particle energy of 30 Mev the corresponding energy width is about 1.0 Mev. Use of maximum selectivity was found to give peaks approximately two-thirds as broad, indicating an actual beam energy spread of perhaps 0.4 Mev, if range straggling in the absorbers is taken into account.

Despite the broadened energy window, the conditions of less-than-maximum energy selectivity were found to give more reliable data. Location of peak positions with an uncertainty of 1 mg/cm² Al or less was easy under these conditions. Under conditions of maximum selectivity, the Al absorber steps were large enough so that the true peak counting rate was often not achieved; further, very slight shifts in beam energy during traversal of a peak caused difficulties.

A possible question concerning the operating conditions actually used is whether alpha particles scattered inelastically with small energy losses were counted in significant numbers. The quite accurate Coulomb dependence of the cross sections at low energies (Sec. III) argues against this possibility. Further evidence is found in the fact that occasional checks made with maximum selectivity showed counting rates of not more than 5 percent of the peak counting rate for energies immediately below the elastic peak energy. Contributions from elastically scattered alphas from surface contaminants such as C and O were shown to be well out of the picture because of the relatively large amounts of energy lost to the light recoil nuclei.

The counters were checked at frequent intervals

¹⁰ Aron, Hoffman, and Williams, U. S. Atomic Energy Commission, Document AECU-663, 1949 (unpublished).

during each run by observing the 8.8-Mev Th C' alpha particles from a Th B source mounted in one of the foil wheels. In this way it was established that the counter efficiency did not change during a run. The natural alpha source was also useful in measuring the Al equivalent of the counter, counter window, and air path, as well as in demonstrating that the cyclotron magnetic field and the intense gamma-ray and neutron fluxes present under operating conditions had no adverse effects upon the counter system.

Because of the directional sensitivity of the counter telescope, it was necessary to correct the data to take into account multiple small-angle scattering in the variable aluminum absorber J (Fig. 1). A correction factor varying by about 10 percent over the extreme energy range 43 to 13 Mev was applied to the data, the efficiency of the counter system being greatest for particles of lowest energy.

Further details of the apparatus and experimental procedures are given elsewhere.¹¹

III. RESULTS AND DISCUSSION

Typical of the results¹² obtained are those for elastic scattering of alpha particles by Pb at 60° in the laboratory system. These results are shown in Fig. 3, in which cross section is plotted against alpha-particle

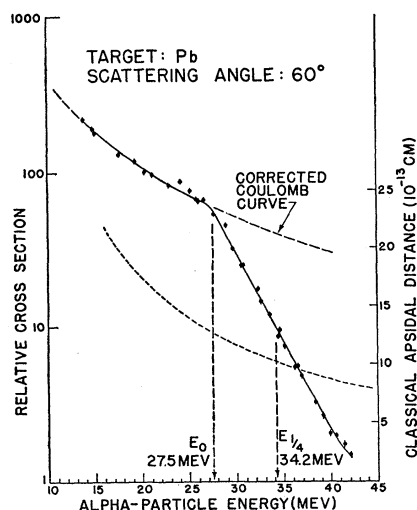


FIG. 3. Elastic scattering of alpha particles by lead at 60° (laboratory system). Cross section (relative) is plotted on a logarithmic scale against alpha-particle energy. The low-energy data are normalized to a corrected Coulomb curve (see text). The critical energy E_0 corresponds to the intercept of the straight-line portion of the experimental curve with the corrected Coulomb curve. At the energy $E_{1/4}$, the experimental cross section is one-quarter of the Coulomb cross section. The lower dashed curve and the scale on the right show the apsidal distance for the classical alpha-particle trajectory as a function of alpha-particle energy.

¹¹ Harvey E. Wegner, thesis, University of Washington, 1953 (unpublished).

¹² Most of these results were first presented at the 1954 Washington meeting of the American Physical Society; see G. W. Farwell and H. E. Wegner, Phys. Rev. **95**, 664(A) (1954).

energy. The alpha-particle energy is that measured by the counter system, and is about 2 percent less than the incident energy because of the energy lost to the recoil nucleus. A logarithmic scale is used for the cross section in order to avoid undue compression of the high-energy part of the curve and to bring out its simple nature.

The "corrected Coulomb curve" shown is normalized to the low-energy experimental data. This curve follows approximately the inverse square dependence of the Coulomb (Rutherford) cross section upon alpha-particle energy, but it is altered slightly to take into account the small variation of scattering angle with energy due to the fringing magnetic field of the cyclotron (Sec. II).

At low energies, the observed cross section follows the Coulomb dependence satisfactorily. At about 27 Mev, however, the cross section begins to drop very rapidly as the alpha-particle energy increases. As in the case of Au (Sec. I), the energy dependence of the cross section over a considerable range of energies is given by the simple empirical formula

$$\sigma(E) = \sigma(E_0) \exp\{-K(E - E_0)\}.$$

The critical energy E_0 corresponds to the intercept of the straight-line portion of the experimental curve with the corrected Coulomb curve. In this case it has the value 27.5 ± 0.3 Mev. The coefficient K is $0.266 \pm 0.006 \text{ Mev}^{-1}$.

The lower dashed curve in Fig. 3 shows the classical apsidal distance as a function of alpha-particle energy. The critical energy E_0 is seen to correspond to an apsidal distance of about 13×10^{-13} cm, a distance much larger than the sum of the accepted values of the Pb nuclear radius ($8-9 \times 10^{-13}$ cm) and the alpha-particle radius ($1-2 \times 10^{-13}$ cm), and it is evident that nuclear effects are strongly felt at somewhat larger distances than might be expected intuitively.

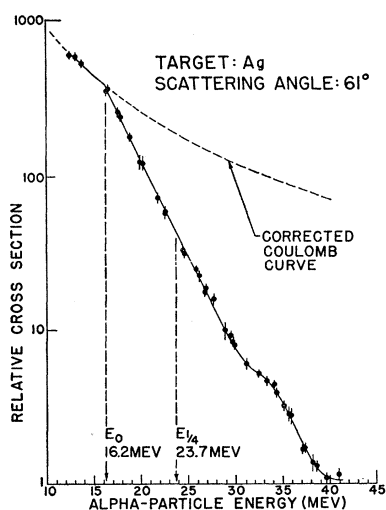


FIG. 4. Elastic scattering of alpha particles by silver at 61° .

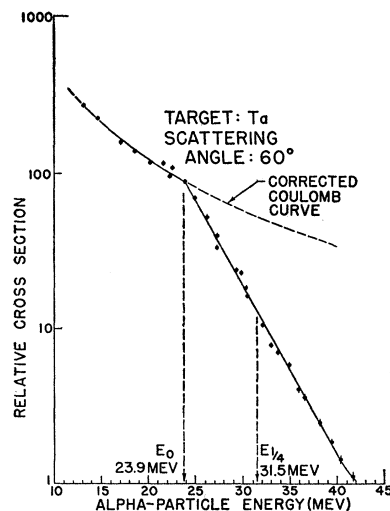


FIG. 5. Elastic scattering of alpha particles by tantalum at 60° .

The significance of the parameter $E_{1/4}$, the energy at which the observed cross section has fallen to one-quarter of the Coulomb cross section, is discussed below (Sec. IV). In the case of Pb, $E_{1/4}$ has the value 34.2 ± 0.4 Mev, corresponding to a classical apsidal distance of about 10.3×10^{-13} cm.

Figures 4, 5, and 6 show the experimental results for Ag, Ta, and Th, respectively.

In the case of Ag (Fig. 4), normalization to the Coulomb curve is less certain than for the other elements studied. Because of the low Coulomb barrier, nuclear effects leading to a rapidly decreasing cross section set in at much lower energies. Another feature which distinguishes the Ag curve is the abrupt shift of the straight-line portion of the curve which takes place between 31 and 35 Mev; this shift is as yet unexplained.

Table I summarizes the results for the parameters E_0 , $E_{1/4}$, and K . For completeness, data⁷ for Au are included, although the experimental curves are not presented in this paper. The probable errors given take into account uncertainties in determination of total range of the scattered particles at each energy and in fitting Coulomb and straight-line curves to the appropriate parts of the experimental data. Allowance for errors in the range-energy curves has not been made; however, such errors should be of the order of 1 percent or less and would affect all results similarly. The values given for K were obtained by means of least squares solutions of the data for the high-energy portions of the curves.

IV. INTERPRETATION

The parameters E_0 , $E_{1/4}$, and K listed in Table I can be measured quite accurately. If a correlation can be made between these parameters and the alpha-particle and nuclear radii, the experiments offer a promising means of obtaining information about nuclear radii.

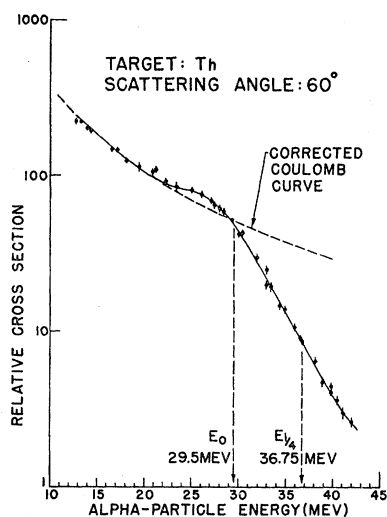


FIG. 6. Elastic scattering of alpha particles by thorium at 60° .

A semiclassical strong absorption model has been used by Blair⁸ to interpret the present experiments. In this model the outgoing l th partial wave is assumed to vanish if the apsidal distance for the corresponding classical trajectory is less than the sum of the radius of the nucleus and the radius of the alpha particle; otherwise it has a phase characteristic of pure Coulomb scattering. The theory predicts that the sum of nuclear and alpha-particle radii is approximately equal to the classical apsidal distance evaluated at the energy for which the experimental cross section is one-quarter of the corresponding Coulomb cross section. It is this energy which is given in Table I as $E_{1/4}$.

Table II gives the classical apsidal distances D_0 and $D_{1/4}$ corresponding to the observed alpha-particle energies E_0 and $E_{1/4}$, respectively. Allowance for the motion of the recoil nucleus has been made in the calculations. The estimated probable errors are based upon the uncertainties in E_0 and $E_{1/4}$ and in the angle of scattering.

As a measure of the consistency of the results and the validity of the interpretation, Table II also lists the values of the quantity $D_{1/4} - R_n$. (The nuclear radii are calculated from $R_n = r_0 A^{1/3}$, with $r_0 = 1.50 \times 10^{-13}$ cm.) According to Blair's interpretation, $R_\alpha = D_{1/4} - R_n$ represents the effective collision radius of the alpha particle and should be the same for all cases. The results for R_α agree within the experimental uncertainties except for the case of Au at 96° , which gives a value slightly larger than the others.

Other values of r_0 give reasonable agreement with the present results if one is willing to accept larger values for the alpha-particle radius. In Fig. 7, the experimental values of $D_{1/4}$ are plotted against $A^{1/3}$. Under the assumption that $D_{1/4} = r_0 A^{1/3} + R_\alpha$, curves are shown for several values of r_0 and R_α . The best fit to the experimental points is given by $r_0 = 1.50$ and $R_\alpha = 1.38$ (units of 10^{-13} cm). Taking $r_0 = 1.35$ and

$R_\alpha = 2.24$ also gives reasonable agreement although the Ag point is then low. For $r_0 = 1.20$, the Ag point is even farther off and the very large value $R_\alpha = 3.10$ is indicated.

In estimating nuclear radii from lifetimes and energies in alpha decay, Blatt and Weisskopf¹³ have assumed an effective alpha-particle radius of 1.2×10^{-13} cm. This gives satisfactory agreement with nuclear radii determined from total neutron cross-section measurements in cases (Pb and Bi) where both types of data are available. Although a radius of 2.24×10^{-13} cm, here corresponding to $r_0 = 1.35 \times 10^{-13}$ cm, would not be unreasonable,¹⁴ it would be difficult to accept the very large values of R_α required by the choice of still smaller values of r_0 .

It should be noted that the one-quarter point interpretation used here is defined most sharply for scattering angles near 90° (see following paper by J. S. Blair). For scattering at 60° , the best theoretical fit to the experimental data is obtained by using radii

TABLE I. Summary of experimental parameters. E_0 is the critical energy above which departures from Coulomb scattering occur. (See also the caption for Fig. 3.) $E_{1/4}$ is the energy at which the observed cross section is one-quarter of the Coulomb cross section. K is the slope parameter for the high-energy part of the curve. Above the critical energy, the cross section follows the energy dependence $\sigma(E) = \sigma(E_0) \exp\{-K(E - E_0)\}$.

Target element	Scattering angle ^a	Z	E_0 (MeV)	$E_{1/4}$ (MeV)	K (MeV ⁻¹)
Ag	61°	47	16.2 ± 0.4	23.7 ± 0.4	0.281 ± 0.004
Ta	60°	73	23.9 ± 0.3	31.5 ± 0.4	0.251 ± 0.004
Au	60°	79	27.0 ± 0.3	33.6 ± 0.4	0.271 ± 0.004
Pb	60°	82	27.5 ± 0.3	34.2 ± 0.4	0.266 ± 0.006
Th	60°	90	29.5 ± 0.4	36.75 ± 0.5	0.246 ± 0.004
Au	96°	79	20.4 ± 0.4	24.9 ± 0.4	0.394 ± 0.010

^a Estimated for the energies near E_0 and $E_{1/4}$. The uncertainty is about $\pm 1^\circ$.

about 0.5×10^{-13} cm larger than those obtained from the one-quarter point recipe. A still larger increase is indicated for the best theoretical fit for silver; since the experimental result is both the lowest (with respect to the general trend) and the least precisely determined, this is not surprising.

The values for the slope parameter K for 60° scattering (Table I) show a slight downward trend with increasing Z . The exception to this trend is Ta. The exception is also visible in the abnormally large value of D_0 for Ta, although $D_{1/4}$ for this element follows the general trend accurately. Since Ta is the only element studied which has a large quadrupole moment, one is tempted to suggest that the Ta nucleus presents a slightly smaller or slightly larger nuclear "radius" to the alpha particle, depending upon its orientation relative to the alpha-particle trajectory. The average

¹³ J. M. Blatt and V. F. Weisskopf, *Theoretical Nuclear Physics* (John Wiley and Sons, Inc., New York, 1952), p. 574.

¹⁴ Reference 13, p. 357.

“radius” is not abnormal, but the steepness of the high-energy $\sigma(E)$ curve is lessened, and nuclear effects are felt at slightly larger distances than would be the case for a spherical nucleus. This possibility will be tested by looking at other elements with large quadrupole moments.

Blair's theoretical curves of cross section *versus* energy⁸ show a slight increase over the Coulomb cross section just before the sudden drop at the critical energy. The experimental curve for Th exhibits such a rise, but it is considerably more spread out than that of the theoretical curve. The Pb and Ta data are not inconsistent with such a rise, but the evidence is considered inconclusive.

V. SUMMARY AND CONCLUSIONS

Cross sections for the elastic scattering of alpha particles by Ag, Ta, Au, Pb, and Th show the same general energy dependence. Up to a certain critical energy E_0 , which increases with Z , the cross section for each element decreases with increasing alpha-

TABLE II. Classical apsidal distances. D_0 and $D_{1/4}$ are the classical apsidal distances corresponding to alpha-particle energies E_0 and $E_{1/4}$, respectively (see Table I). $D_{1/4}-R_n$ may be interpreted as the effective radius of the alpha particle (see text).

Target element	Scattering angle	A	D_0 (10^{-13} cm)	$D_{1/4}$ (10^{-13} cm)	R_n^a (10^{-13} cm)	$D_{1/4}-R_n$ (10^{-13} cm)
Ag	61°	107.9	12.2 ± 0.4	8.3 ± 0.3	7.14	1.2 ± 0.3
Ta	60°	180.9	13.05 ± 0.21	9.90 ± 0.16	8.48	1.42 ± 0.16
Au	60°	197.2	12.50 ± 0.20	10.05 ± 0.16	8.73	1.32 ± 0.16
Pb	60°	207.2	12.76 ± 0.21	10.26 ± 0.17	8.88	1.38 ± 0.17
Th	60°	232.1	13.06 ± 0.21	10.48 ± 0.17	9.22	1.26 ± 0.17
Au	96°	197.2	12.76 ± 0.35	10.45 ± 0.25	8.73	1.72 ± 0.25

^a Nuclear radius calculated from $R_n = r_0 A^{1/3}$, with $r_0 = 1.50 \times 10^{-13}$ cm.

particle energy in agreement with the Rutherford formula. At higher energies, the cross section drops sharply with increasing energy and can be represented over a considerable energy range by the simple empirical formula $\sigma(E) = \sigma(E_0) \exp\{-K(E-E_0)\}$. The slope parameter K appears to decrease slightly with increasing Z , although the value of K for Ta is out of line with this trend.

Analysis of the elastic scattering problem in terms of a semiclassical strong absorption model leads to the

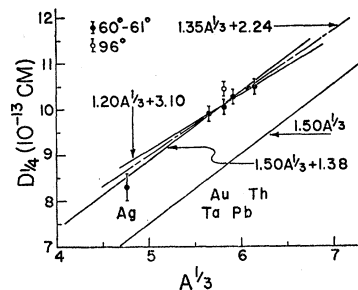


FIG. 7. Classical apsidal distance $D_{1/4}$, which in the strong absorption model represents the sum of nuclear and alpha-particle radii, is plotted against $A^{1/3}$. Under the assumption that $D_{1/4} = r_0 A^{1/3} + R_n$, the best fit to the experimental data is given by $r_0 = 1.50$ and $R_n = 1.38$ (units of 10^{-13} cm).

conclusion that the experimental cross section should be equal to one-quarter of the Coulomb (Rutherford) cross section at the alpha-particle energy for which the classical apsidal distance $D_{1/4}$ is equal to the sum of the nuclear and alpha-particle radii.

Assuming $D_{1/4} = r_0 A^{1/3} + R_n$, the best fit for the experimental data is given by $r_0 = 1.50 \times 10^{-13}$ cm, $R_n = 1.38 \times 10^{-13}$ cm. Values of r_0 less than 1.35×10^{-13} cm lead to poor fits to the experimental data and to unreasonably large values for the alpha-particle radius.

More data are needed at both higher and lower Z . Going to lower Z requires observation at smaller scattering angles in order to include a region of pure Coulomb scattering. It is also desirable to test the theoretical interpretation of the results by observations on the present target materials at angles other than 60° , since the indicated nuclear radii should be independent of the scattering angle. Preparations are being made for these experiments.

VI. ACKNOWLEDGMENT

We are indebted to Dr. J. S. Blair for many valuable discussions concerning the progress of the experimental work and the theoretical interpretation of the results. Thanks are also due Mr. T. J. Morgan and other members of the cyclotron group, particularly Mr. D. D. Kerlee, Mr. D. J. Farmer, and Mr. J. R. Penning, for their assistance in cyclotron operation and construction of experimental equipment.